The Binding of Inosine Monophosphate to *Escherichia coli* Carbamoyl Phosphate Synthetase*

James B. Thoden‡, Frank M. Raushel§, Gary Wesenberg‡, and Hazel M. Holden‡¶

From the ‡Department of Biochemistry, College of Agricultural and Life Sciences, University of Wisconsin, Madison, Madison, Wisconsin 53705 and the §Department of Chemistry, Texas A&M University, College Station, Texas 77843

Carbamoyl phosphate synthetase (CPS) from *Escherichia coli* catalyzes the formation of carbamoyl phosphate, which is subsequently employed in both the pyrimidine and arginine biosynthetic pathways. The reaction mechanism is known to proceed through at least three highly reactive intermediates: ammonia, carboxyphosphate, and carbamate. In keeping with the fact that the product of CPS is utilized in two competing metabolic pathways, the enzyme is highly regulated by a variety of effector molecules including potassium and ornithine, which function as activators, and UMP, which acts as an inhibitor. IMP is also known to bind to CPS but the actual effect of this ligand on the activity of the enzyme is dependent upon both temperature and assay conditions. Here we describe the three-dimensional architecture of CPS with bound IMP determined and refined to 2.1 Å resolution. The nucleotide is situated at the C-terminal portion of a five-stranded parallel β-sheet in the allosteric domain formed by Ser^{937} to Lys^{1073}. Those amino acid side chains responsible for anchoring the nucleotide to the polypeptide chain include Lys^{954}, Thr^{974}, Thr^{977}, Lys^{993}, Asn^{1015}, and Thr^{1017}. A series of hydrogen bonds connect the IMP-binding pocket to the active site of the large subunit known to function in the phosphorylation of the unstable intermediate, carbamate. This structural analysis reveals, for the first time, the detailed manner in which CPS accommodates nucleotide monophosphate effector molecules within the allosteric domain.

Carbamoyl phosphate synthetase (CPS)[1] is one of the few allosterically regulated enzymes whose three-dimensional structure is now known to high resolution (1, 2). A list of other regulated proteins, whose molecular architectures are known in quite extensive detail, includes phosphofructokinase (3), aspartate transcarbamoylase (4), glutamine synthetase (5), and glycogen phosphorylase (6), among others. The biochemical role of CPS is to catalyze the formation of carbamoyl phosphate, an

[1] The abbreviation used is: CPS, carbamoyl phosphate synthetase.

unstable precursor that initiates subsequent steps in the biosynthesis of both pyrimidine nucleotides and arginine. The end-product of the pyrimidine biosynthetic pathway, UMP, allosterically *inhibits* this enzyme. Conversely, ornithine, the co-substrate with carbamoyl phosphate in the next step of the arginine biosynthetic pathway, *enhances* the catalytic activity of CPS. Each of these effectors primarily, but not exclusively, modulates the activity of CPS by raising or lowering the dissociation constant for Mg^{2+}ATP by approximately one order of magnitude (7, 8).

As isolated from *E. coli*, CPS is a large multidomain heterodimeric protein. The smaller of the two subunits has a molecular weight of ~42,000 and is catalytically responsible for the hydrolysis of glutamine and the subsequent translocation of the ammonia product to the large subunit (9). The larger subunit (molecular weight ~118,000) is composed of four major regions as indicated in Fig. 1 (1, 10). Two of these structural units, known as the carboxyphosphate (Met^1-Glu^{403}) and carbamoyl phosphate (Asn^{554}-Asn^{936}) synthetic components are homologous to one another and contain all of the catalytic machinery necessary for the final assembly of carbamoyl phosphate. These two synthetase units are linked together by a third domain (Val^{404}-Ala^{553}) whose functional role in the structure and catalytic properties of CPS is still not well understood. However, this region of the protein appears to play a role in the oligomerization of the α,β-heterodimer into an $(\alpha,\beta)_4$-tetrameric species (1). The remaining domain (Ser^{937}-Lys^{1073}) has been shown by both x-ray crystallographic and biochemical methods to harbor the binding sites for such allosteric effectors as ornithine, UMP, and IMP.

The binding site for the positive allosteric effector, ornithine, was identified in the original x-ray structural analysis of CPS (1, 2). Ornithine was found to straddle the interface between the allosteric domain and the carbamoyl phosphate synthetic component. Specifically, the α-amino group of this compound was shown to lie within hydrogen bonding distance to O$^\gamma$ of Tyr^{1040} in the allosteric domain, whereas the δ-amino group was positioned within 3.0 Å from the carboxylate groups of Glu^{783} and Glu^{892}, and O of Asp^{791}, all of which originate from the carbamoyl phosphate synthetic component. In addition, the carboxylate group of ornithine was observed interacting with both the backbone amide nitrogen and O$^\gamma$ of Thr^{1042}. This same structure of CPS also provided the first hint for the locations of the nucleotide monophosphate binding sites. Indeed, within the allosteric domain, an inorganic phosphate was observed, hydrogen bonded, and ion-paired to Lys^{954}, Thr^{974}, Thr^{977}, and Lys^{993}. The hydroxyl group of Thr^{977} had previously been shown to be critical for the display of the allosteric properties of UMP (11), although somewhat later Lys^{993} was shown to be the residue modified upon photolabeling CPS with UMP (12). From the above mentioned data, a structural model was subsequently proposed by Thoden *et al.* (1) for the binding of UMP or

This paper is available on line at http://www.jbc.org

FIG. 1. **Space-filling representation of the CPS α,β-heterodimer.** The N-terminal and C-terminal domains of the small subunit are color coded in *magenta* and *purple*, respectively. Met[1] to Glu[403], Val[404] to Ala[553], Asn[554] to Asn[936], and Ser[937] to Lys[1073] of the large subunit are displayed in *green*, *yellow*, *blue*, and *red*, respectively.

TABLE I
Intensity Statistics

	Overall	30.0–4.52	3.59	3.14	2.85	2.65	2.49	2.37	2.26	2.18	2.10
						Å					
Number of independent reflections	445,013	48,775	47,831	47,563	46,535	45,669	44,693	43,473	42,158	39,899	38,417
Redundancy	4.0	7.0	7.0	6.3	3.5	3.3	3.1	2.9	2.7	2.5	2.3
Percent completeness	93	100	100	100	100	96	94	92	90	84	81
Avg I/avg σ (I)	30.3	48.0	52.8	43.4	25.6	18.5	13.2	9.3	7.0	5.2	3.9
R-factor (%)[a]	5.0	3.9	4.5	5.8	6.3	7.8	9.9	12.5	15.1	19.3	22.1

Resolution range spans the header columns from 30.0–4.52 to 2.10.

[a] R-factor = $(\Sigma|I - \bar{I}|/\Sigma I) \times 100$.

TABLE II
Least squares refinement statistics

Resolution limits (Å)	30.0–2.1
$R_{overall}$ (%)[a]	19.3
R_{free} (%)	25.7
No. of reflections used	444,816
No. of protein atoms	44,374
No. of water molecules	4037
Weighted root mean square deviations from ideality	
Bond length (Å)	0.013
Bond angle (deg)	2.30
Planarity (trigonal) (Å)	0.005
Planarity (other planes) (Å)	0.009
Torsional angle (degrees)[b]	17.9

[a] R-factor = $\Sigma|F_o - F_c|/\Sigma|F_o|$ where F_o is the observed structure-factor amplitude, and F_c is the calculated structure-factor amplitude.
[b] The torsional angles were not restrained during the refinement.

IMP to the allosteric domain of the large subunit.

Relative to UMP, the allosteric properties exhibited by IMP are rather modest. Originally, IMP was described as an activator of CPS (13–15) but Reinhart and colleagues (7) elegantly demonstrated that the net allosteric effects of IMP can be modulated by temperature. At high temperatures, IMP activates CPS, whereas at lower temperatures the enzymatic activity is depressed. From past investigations (13, 14, 16), it was suggested that both IMP and UMP compete for the same binding site. More recently, it has been demonstrated quantitatively that the allosteric effects exhibited by IMP and UMP are strictly competitive with one another (17). These results are fully consistent with a common binding site for these two nucleotide monophosphate molecules. In contrast, ornithine and either IMP or UMP can bind simultaneously to CPS but the activation properties of ornithine completely dominate the inhibitory effects of either IMP or UMP (17).

Here we report the first structural analysis of the nucleotide monophosphate allosteric binding site for CPS from *E. coli*. For this investigation, CPS was crystallized in the presence of both IMP and ornithine. The IMP binding site was found to be contained wholly within the allosteric domain of CPS in a position consistent with previous biochemical data. The model presented here provides one snapshot along the way toward a more complete structural understanding of the allosteric behavior displayed by this remarkable enzyme.

EXPERIMENTAL PROCEDURES

Purification and Crystallization Procedures—Protein employed in this investigation was purified as described previously (18). For crystallization trials, the protein was concentrated to 4 mg/ml in 10 mM HEPES (pH 7.0) and 100 mM KCl. Large single crystals were grown at 4 °C using a precipitant solution containing 0.65 M tetraethylammonium chloride, 8% w/v (polyethylene) glycol 8000, 100 mM KCl, 0.5 mM MnCl₂, 0.5 mM ornithine, 1.25 mM ADP, 1.25 mM BeF₃, 5.0 mM IMP, and 25 mM HEPES (pH 7.4). The crystals took approximately 3 months to achieve maximum dimensions of $1.2 \times 0.5 \times 0.4$ mm. As in previous structural analyses of CPS from *E. coli*, these crystals belonged to the space group P2₁2₁2₁ with unit cell dimensions of $a = 152.1$ Å, $b = 163.9$ Å, and $c = 331.2$ Å and one $(\alpha,\beta)_4$-heterotetramer per asymmetric unit.

X-ray Data Collection and Processing—Before x-ray data collection, the crystals were transferred to a cryoprotectant solution as described previously and subsequently flash-cooled to -150 °C in a stream of nitrogen gas (2). X-ray data to 2.1 Å resolution were collected at the Stanford Synchrotron Radiation Laboratory on beam-line 7–1 with the MAR300 image plate system. A low resolution x-ray data set, consisting of eighty "1°" frames with the direct beam centered on the detector and a crystal-to-detector distance of 420 mm, was collected first. These frames were collected with a constant number of photons per frame. The detector was then translated up into its offset position, again at a crystal-to-detector distance of 420 mm. A total of 320 "0.7°" frames was

FIG. 2. **Electron density corresponding to the IMP moiety.** The electron density shown was calculated with coefficients of the form $(F_o - F_c)$ and contoured at 3 σ. The portion of the polypeptide chain responsible for forming the IMP binding pocket in the allosteric domain is indicated by the ribbon representation.
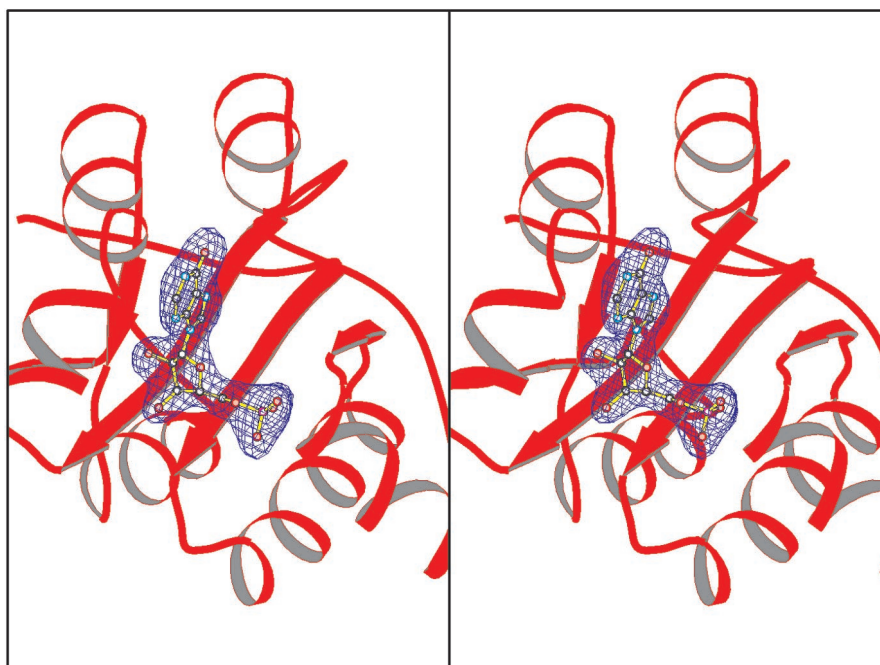
collected. These frames were processed with DENZO and scaled with SCALEPACK (19). From 3,249,722 measurements, 1,855,323 reflections were integrated and reduced to 445,013 unique reflections after scaling. Scaling statistics are presented in Table I.

The structure of the CPS·IMP complex described here was solved by the technique of molecular replacement (20) with the software package AMORE (21) and using, as a search model, the complete tetrameric form of CPS previously refined to 2.1 Å resolution (2). Following rigid body refinement, the model was subjected to least squares refinement at 2.1 Å resolution with the software package TNT (22). Because there were over 5,800 amino acid residues in the asymmetric unit, the model building and refinement processes were expedited by averaging the electron densities corresponding to the four α,β-heterodimers in the asymmetric unit as described previously (23). Alternate cycles of rebuilding using this averaged electron density map followed by least squares refinement of the "averaged" model expanded back into the unit cell reduced the R_{cryst} to 20.8% and the R_{free} to 26.5%. For calculation of R_{free}, 5% of the x-ray data were removed from the reflection file. At this point the entire tetrameric model was adjusted in the unit cell and an additional cycle of least squares refinement conducted leading to an R_{cryst} of 19.2% and an R_{free} of 25.7%. A final cycle of refinement was conducted with all measured x-ray data from 30 to 2.1 Å resulting in an R-factor of 19.3%. Relevant refinement statistics are presented in Table II. The CPS·IMP model described here includes eight ADP molecules, 12 manganese ions, 8 ornithines, 4 inorganic phosphates, 28 potassium ions, 12 chloride ions, 4,037 water molecules, 4 tetraethylammonium ions, and 4 IMP molecules. The following side chains were modeled as multiple conformations: Ser[29], Arg[130], Glu[278], Asp[416], Glu[655], Glu[910], Gln[967], and Glu[983] in the large subunit and Arg[215] in the small subunit of α,β-heterodimer I; Arg[145] in the large subunit and Met[286] in the small subunit of α,β-heterodimer II; Arg[82], Arg[222], Arg[490], Arg[559], Glu[591], Lys[634], Gln[645], Arg[652], Glu[771], Lys[941], Glu[1009], and Arg[1021] in the large subunit and Gln[78] in the small subunit of α,β-heterodimer III and Lys[35] and Glu[478] in the large subunit of α,β-heterodimer IV. In addition, Cys[269] was modeled as sulfenic acid for all four small subunits contained within the asymmetric unit.

RESULTS AND DISCUSSION

The CPS crystals employed in this investigation contained a complete $(\alpha,\beta)_4$-heterotetramer in the asymmetric unit. Because the four (α,β)-heterodimers are strikingly similar, however, the following discussion will refer only to (α,β)-heterodimer II as deposited in the Brookhaven Protein Data Bank. Shown in Fig. 2 is the electron density corresponding to the IMP ligand. The nucleotide fits the electron density best with the ribose in the $C_{2'}$-*endo* conformation. The purine ring adopts an anti-orientation and is tilted by approximately 156° from

the plane of the ribose ring. This is in sharp contrast to those conformations observed for the ADP moieties bound to CPS whereby the bases are tilted by approximately 128° and the ribose rings adopt $C_{3'}$-*endo* puckers. All the nucleotide monophosphates contained within the crystallographic asymmetric unit are very well ordered with the IMP bound to (α,β)-heterodimer II having an average temperature factor of 30.5 Å^2.

The allosteric domain of CPS (Ser[937] to Lys[1073]) is characterized by a five-stranded parallel β-sheet flanked on either side by two and three α-helices, respectively. As can be seen in Fig. 2, the IMP ligand is situated at the C-terminal end of this sheet and, indeed, is completely contained within the allosteric domain as originally predicted (1). A close-up view of the IMP binding pocket is displayed in Fig. 3a and a cartoon of potential hydrogen bonds between the ligand and the protein is shown in Fig. 3b. As indicated by the gray spheres in Fig. 3a, there are three water molecules located within a 5 Å sphere of the purine nucleotide. One side of the hypoxanthine ring is packed against a fairly hydrophobic pocket formed by Ile[1001], Val[1028], and Ile[1029]. The only direct electrostatic contact between the purine base and the protein occurs between O-6 of the hypoxanthine ring and N of Val[994]. A water molecule is located within 3.0 Å to N-1 of the purine base. Both $N^{\delta 2}$ of Asn[1015] and O^{γ} of Thr[1017] serve to anchor the 2'-OH group of the ribose to the protein. The 3'-OH group of the ribose lies within hydrogen bonding distance to O of Thr[1016]. All three phosphoryl oxygens form direct hydrogen bonds with the protein via the side chain functional groups of Lys[954], Thr[974], Thr[977], and Lys[993] as indicated by the dashed lines in Fig. 3b. In addition, the backbone amide groups of Gly[976] and Thr[977] also lie within hydrogen bonding distance to two of the phosphoryl oxygens. Approximately 90% of the surface area for the nucleotide ligand is buried upon binding to CPS as calculated with the program GRASP and employing a search radius of 1.4 Å (24).

The original structure of CPS was solved in the presence of both Mn^{2+}ADP and ornithine to 2.8 Å resolution (1). In that model, two ornithine binding sites per α,β-heterodimer were identified. The first ornithine was shown to bridge the C-domain of the carbamoyl phosphate synthetic component to the allosteric domain. The second ornithine, along with an inorganic phosphate, was positioned at the C-terminal end of the
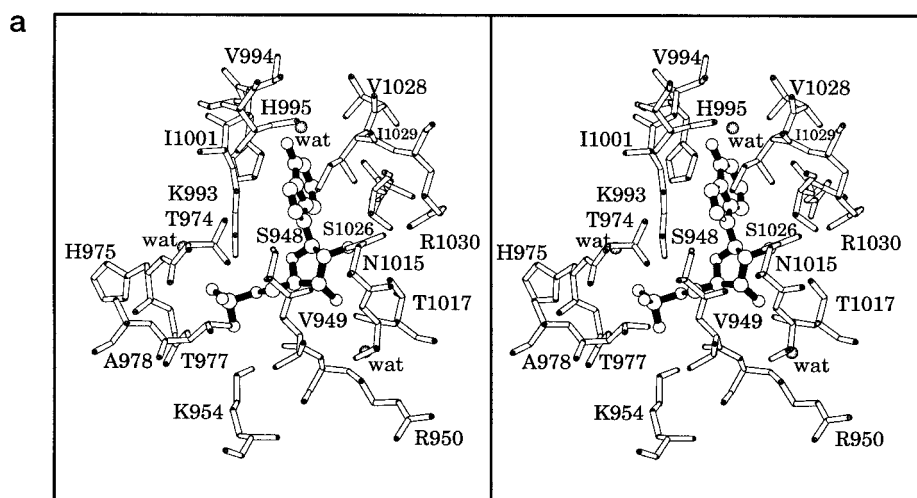
a

FIG. 3. **The IMP binding pocket.** *Panel a*, a close-up view of those amino acid residues located within approximately 5 Å of atoms of the IMP. *Panel b*, a cartoon of potential hydrogen bonds between the ligand and the protein, as indicated by the *dashed lines*.
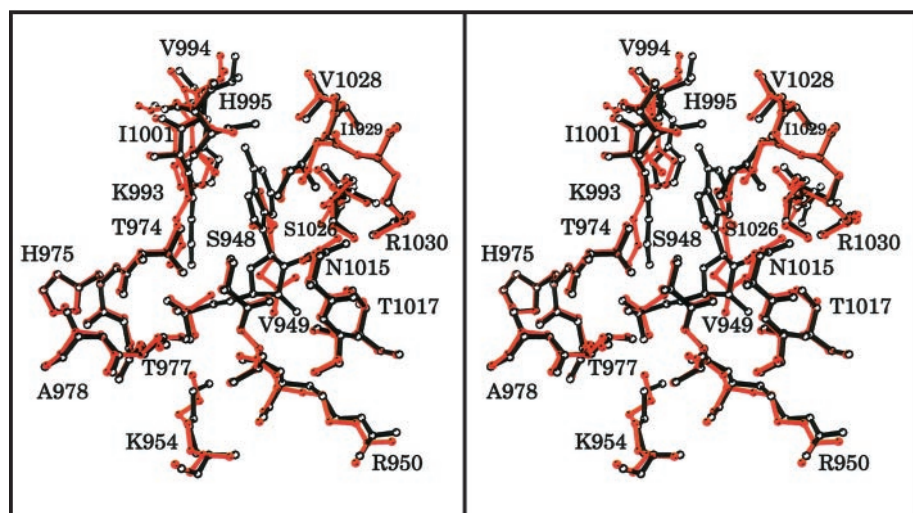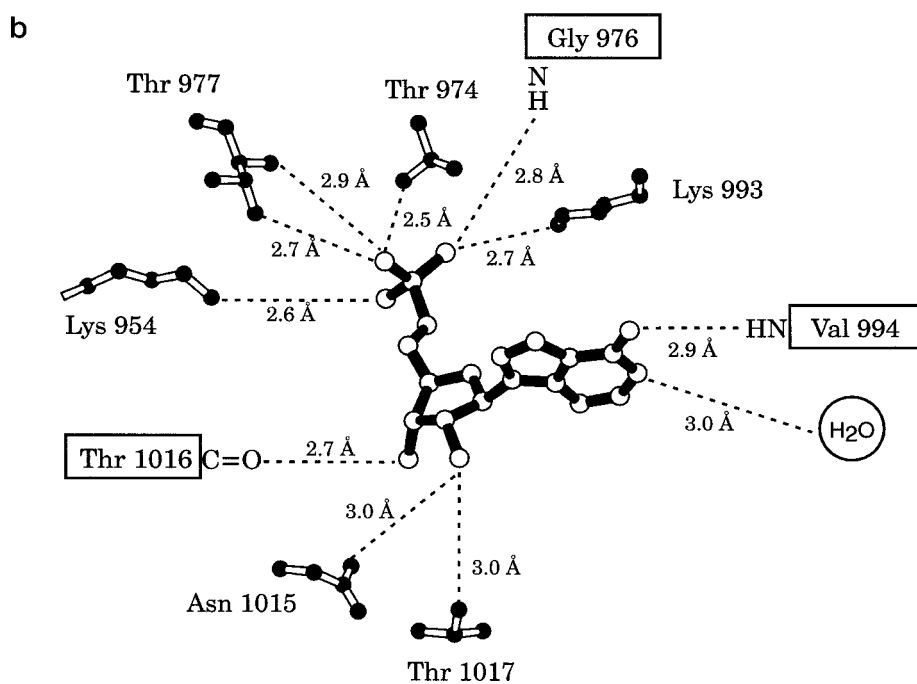
b

FIG. 4. **Superposition of the CPS allosteric binding pockets with bound IMP or glutamine/inorganic phosphate.** The model described in this report is shown in *black*, whereas the structure of CPS complexed with glutamine and inorganic phosphate, as described by Thoden *et al.* (2), is displayed in *red*. Note the nearly exact correspondence between the inorganic phosphate and the phosphoryl moiety of the nucleotide.

β-sheet in the allosteric domain. At that time, it was postulated that the combination of ornithine and inorganic phosphate was most likely mimicking the mode of binding for such nucleotide ligands as UMP and IMP. For the subsequent x-ray data collection and analysis of the CPS model to 2.1 Å resolution, the crystals were first soaked in a solution containing 25 mM glu-

FIG. 5. **α-Carbon trace of the CPS α,β-heterodimer.** The relative disposition of the three active sites and the allosteric effector binding pockets for CPS are indicated by the ball-and-stick representations. The active site for the small subunit is approximately 45 Å from the first Mn^{2+}ADP binding site of the large subunit which, in turn, is 35 Å from the second Mn^{2+}ADP binding motif. This second active site of the large subunit is positioned approximately 14 Å from the ornithine and 19 Å from the IMP ligands.
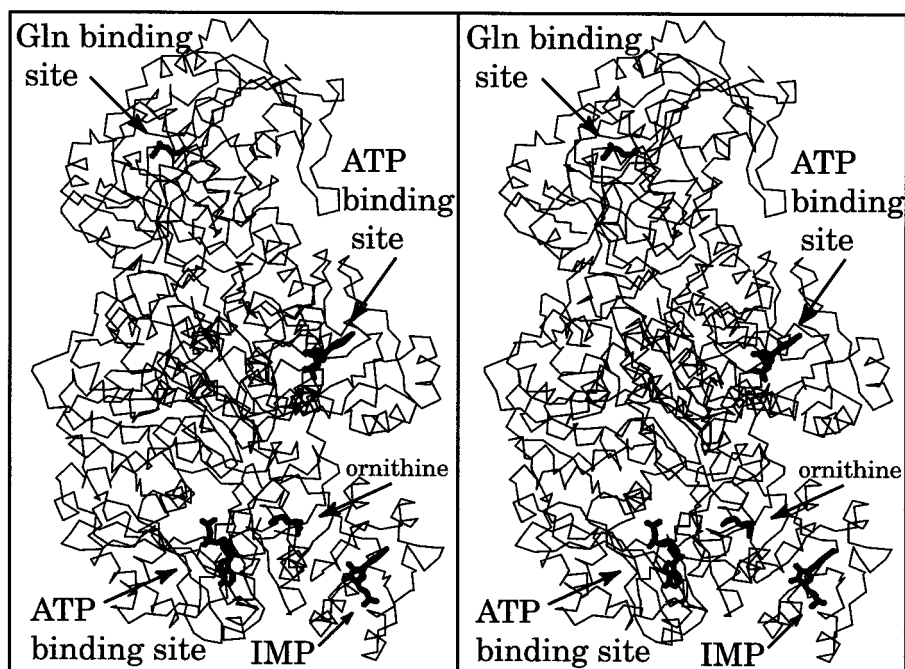
tamine in an attempt to label the active site of the small subunit. Although the glutamine did not bind in the active site in this study, it did, however, displace the ornithine from its binding pocket in the allosteric domain (2).

A superposition of this ligand binding site, as observed in the refined structure of CPS, onto the present CPS·IMP model is depicted in Fig. 4. The phosphoryl group of the nucleotide occupies a nearly identical position to that observed for the inorganic phosphate. This phosphate binding region is positioned at the N-terminal region of an α-helix formed by Thr^{974} to Gly^{982}. It can thus be speculated that both hydrogen bonds and electrostatic interactions with the positive end of the helix dipole serve to promote binding of phosphate moieties to this region of the allosteric domain. The only two side chains that adopt significantly different conformations between the two models are Ile^{1001} and Ile^{1029} where their dihedral angles differ by approximately 120–130°. Other than these side chains, the two CPS complexes are remarkably similar, such that 5,744 of their backbone atoms coincide with a root mean square deviation of 0.31 Å. Recently, Bueso *et al.* (25) demonstrated that IMP bound to CPS can be photocrosslinked to the large subunit in very low yield. The only amino acid residue labeled after photoirradiation was shown to be His^{995}. Site-directed mutagenesis of His^{995} to an alanine residue had relatively little effect on either the catalytic or regulatory properties of CPS. In the crystal structure of the CPS·IMP complex reported here, the imidazole ring of His^{995} is approximately 4 Å from the hypoxanthine ring of the nucleotide monophosphate. The biochemical results of Bueso *et al.* (25) are thus entirely consistent with the fact that His^{995} does not significantly contribute to the binding site for IMP.

In CPS, the IMP ligand binds to the C-terminal portion of a parallel β-sheet. A search of the Brookhaven Protein Data Bank reveals that other enzymes have been solved in the presence of IMP, or analogs thereof, including adenoylsuccinate synthetase (26). Detailed x-ray crystallographic analyses of this enzyme have demonstrated that the IMP ribose adopts the $C_{2'}$-*endo* pucker with the purine base oriented similarly to that observed in CPS (26). Additionally, the phosphoryl group of the nucleotide is positioned within approximately 5 Å of the N-terminal end of an α-helix formed by Gly^{132} to Ala^{142}. The IMP

moiety is deeply buried within the protein such that only about 1% of its surface area is exposed to the solvent. Unlike that observed in CPS, the purine ring makes numerous hydrogen bonding contacts with the protein. Note that adenoylsuccinate synthetase catalyzes the production of adenoylsuccinate from IMP, aspartate, and GTP, and in this case, the nucleotide monophosphate is a true substrate. With regard to the role of IMP acting solely as an effector molecule, however, the only other observed structural example of IMP binding within an allosteric pocket is that of glycogen phosphorylase (27). In this enzyme, the ribose of the nucleotide adopts the $C_{3'}$-*endo* pucker. The ligand is positioned in a rather open region of the molecule with approximately 48% of its surface area exposed to the solvent, the hypoxanthine ring facing outwards and no direct protein contacts to the base. Other than the similarities in ribose puckers between CPS and adenoylsuccinate synthetase, the tertiary motifs employed for IMP binding in these three enzymes are quite different.

The overall spatial relationships between the active sites of the small and large subunits of CPS and the IMP and ornithine effector binding pockets are depicted in Fig. 5. The ornithine and IMP binding sites are separated by approximately 12 Å, whereas the ornithine binding region and active site in the carbamoyl phosphate synthetic component are situated approximately 14 Å apart. Previously, it was demonstrated that allosteric ligands such as IMP and ornithine affect the carbamoyl phosphate-dependent ATP synthesis reaction more so than the other two partial reactions catalyzed by CPS (7). The manner in which the IMP allosteric effector site communicates to this Mg^{2+}ATP binding site is most likely via a complicated series of hydrogen bonds. As an example, there is a hydrogen bonding pathway leading directly from the 2′-hydroxyl group of the IMP ribose to one of the phosphoryl oxygens of the Mn^{2+}ADP. This hydrogen bonding network initiates via the interaction between $N^{δ2}$ of Asn^{1015} and the 2′-hydroxyl group of IMP (Fig. 3b). The backbone amide group of Asn^{1015} interacts with O of Asp^{1041}. In this region, $O^{γ}$ of Thr^{1042} forms a hydrogen bond with the carboxylate group of ornithine. In turn, the δ-amino group of ornithine lies within hydrogen bonding distance to O of Asp^{791}, whereas the backbone amide group of Asp^{791} interacts with O of His^{788}. Finally, the imidazole side

chain of His[788] hydrogen bonds to a phosphoryl oxygen of the $Mn^{2+}ADP$ moiety. Examination of the CPS·IMP complex model described in this report demonstrates that additional hydrogen bonding networks may also exist between the IMP binding pocket and the active site of the carbamoyl phosphate synthetic component.

From previous biochemical studies (13, 14, 16), it is known that IMP and UMP compete for the same binding site on CPS. It can thus be speculated that the structure of CPS described here reveals not only the manner in which IMP is accommodated on the enzyme but also the mode of UMP binding to the allosteric domain, at least as far as the phosphoryl and sugar moieties are concerned. Recent detailed kinetic analyses of the behavior of CPS in the presence of IMP, UMP, or ornithine or combinations thereof have revealed a quite complicated set of catalytic behaviors (17). In addition, these studies have demonstrated that though both ornithine, an activator, and UMP, an inhibitor, can bind simultaneously to CPS, the activating effect of ornithine on the catalytic activity of CPS clearly prevails. What is not apparent from the present structural studies is the manner in which the enzyme discriminates between UMP and IMP. It would appear likely that the same molecular contacts are made to the ribose-phosphate moieties of UMP and IMP in the bound complexes. However, in the structure of IMP complexed to CPS, relatively few contacts are made to the hypoxanthine ring system. We anticipate that a significant molecular rearrangement occurs upon the binding of UMP to CPS that is not observed in the present model. These structural manifestations can only be elucidated via a combination of biochemical and x-ray crystallographic experiments and, indeed, these investigations are in progress.

REFERENCES

1. Thoden, J. B., Holden, H. M., Wesenberg, G., Raushel, F. M., and Rayment, I. (1997) *Biochemistry* **36,** 6305–6316
2. Thoden, J. B., Raushel, F. M., Benning, M. M., Rayment, I., and Holden, H. M. (1999) *Acta Crystallogr. Sec. D.* **55,** 8–24
3. Schirmer, T., and Evans, P. R. (1990) *Nature* **343,** 140–145, and references therein
4. Kosman, R. P., Gouaux, J. E., and Lipscomb, W. N. (1993) *Proteins Struct. Funct. Genet.* **15,** 147–176, and references therein
5. Liaw, S. H., Jun, G., and Eisenberg, D. (1994) *Biochemistry* **33,** 11184–11188, and references therein
6. Gregoriou, M., Noble, M. E., Watson, K. A., Garman, E. F., Krulle, T. M., de la Fuente, C., Fleet, G. W., Oikonomakos, N G., and Johnson, L. N. (1998) *Protein Sci.* **7,** 915–927, and references therein
7. Braxton, B. L., Mullins, L. S., Raushel, F. M., and Reinhart, G. D. (1992) *Biochemistry* **31,** 2309–2316
8. Braxton, B. L., Mullins, L. S., Raushel, F. M., and Reinhart, G. D. (1996) *Biochemistry* **35,** 11918–11924
9. Matthews, S. L., and Anderson, P. M. (1972) *Biochemistry* **11,** 1176–1183
10. Trotta, P. P., Burt, M. E., Haschemeyer, R. H., and Meister, A. (1971) *Proc. Natl. Acad. Sci. U. S. A.* **68,** 2599–2603
11. Czerwinski, R. M., Mareya, S. M., and Raushel, F. M. (1995) *Biochemistry* **34,** 13920–13927
12. Cervera, J., Bendala, E., Britton, H. G., Bueso, J., Nassif, Z., Lusty, C. J., and Rubio, V. (1996) *Biochemistry* **35,** 7247–7255
13. Boettcher, B., and Meister, A. (1981) *J. Biol. Chem.* **256,** 5977–5980
14. Boettcher, B., and Meister, A. (1982) *J. Biol. Chem.* **257,** 13971–13976
15. Kasprzak, A. A., and Villafranca, J. J. (1988) *Biochemistry* **27,** 8050–8056
16. Anderson, P. M. (1977) *Biochemistry* **16,** 587–593
17. Braxton, B. L., Mullins, L. S., Raushel, F. M., and Reinhart, G. D. (1999) *Biochemistry* **38,** 1394–1401
18. Miran, S. G., Chang, S. H., and Raushel, F. M. (1991) *Biochemistry* **30,** 7901–7907
19. Otwinowski, Z. (1993) in *Proceedings of the CCP4 Study Weekend*: *Data Collection and Processing, Oscillation Data Reduction Program* (Sawyer, L., Isaacs, N., and Bailey, S., eds) pp. 56–62, SERC Daresbury Laboratory, United Kingdom
20. Rossmann, M. G. (1972) *The Molecular Replacement Method*, Gordon and Breach Science Publishers, Inc., New York
21. Navaza, J. (1994) *Acta Crystallogr. Sec. A* **50,** 157–163
22. Tronrud, D. E., Ten Eyck, L. F., and Matthews, B. W. (1987) *Acta Crystallogr. Sect. A* **43,** 489–501
23. Thoden, J. B., Miran, S. G., Phillips, J. C., Howard, A. J., Raushel, F. M., and Holden, H. M. (1998) *Biochemistry* **37,** 8825–8831
24. Nicholls, A., Sharp, K. A., and Honig, B. (1991) *Proteins Struct. Funct. Genet.* **11,** 281–296
25. Bueso, J., Cervera, J., Fresquet, V., Marina, A., Lusty, C. J., and Rubio, V. (1999) *Biochemistry* **38,** 3910–3917
26. Poland, B. W., Fromm, H. J., and Honzatko, R. B. (1996) *J. Mol. Biol.* **264,** 1013–1027
27. Oikonomakos, N. G., Zographos, S. E., Tsitsanou, K. E., Johnson, L. N., and Acharya K. R. (1996) *Protein Sci.* **5,** 2416–2428

PROTEIN CHEMISTRY AND STRUCTURE:

The Binding of Inosine Monophosphate to
Escherichia coli **Carbamoyl Phosphate**
Synthetase

James B. Thoden, Frank M. Raushel, Gary
Wesenberg and Hazel M. Holden